Thermal data analysis for urban climate research: A case study of Olomouc, Czechia

Tomáš POUR, Vít VOŽENÍLEK

***Abstract**: Due to the recent advancements in thermal camera technology, it is easier than ever to acquire information about surface temperature in very-high or extreme spatial resolution from manned or unmanned airborne vehicles. The main objective of the paper is to investigate the possibilities of extreme resolution thermal data for urban climate research. The main dataset used for the work is thermal mosaic acquired by an aeroplane above the city of Olomouc in the morning and afternoon on 10th July 2016. The spatial resolution of the dataset fluctuates between 90 and 100 cm per pixel edge. Auxiliary data used for the analysis included open data from European programmes Urban Atlas and CORINE Land Cover. For further analysis, building height information, material type and Local Climate Zones classification were used. The results show a possible comparison in various neighbourhoods and material types while maintaining reference units – Urban Atlas/CORINE Land Cover classes or Local Climate Zones. Verticality analysis shows a significant difference between ground and rooftop levels that need to be taken into account when investigating heat for quality of life. All the analyses confirmed knowledge about the difference between natural and artificial surfaces that most artificial surfaces tend to heat up much more during daytime and fail to cool down completely during the night-time. Moreover, this research lays the foundation to future urban climate research based on extreme resolution thermal images over multiple areas or during long-lasting campaigns.*

***Keywords:** remote sensing, thermal data, urban climate, spatial analysis*

Introduction

The surface temperature plays a crucial role in the research of the urban climate. Air mass above the ground is highly affected by the surface temperature as well as energy balance and the internal climate inside buildings. Human interception and urbanisation in the landscape led to a general trend of increasing temperature of both air mass and the surface in the urban climate. These phenomena are described as the Urban Heat Island (UHI) and Surface Urban Heat Island (SUHI). UHI effect is described as warmer environment in urban areas than in its surrounding rural area. SUHI is a complementary effect regarding the use of artificial materials that are prone to heating up on contrary to natural land cover classes. UHIs are most often monitored using ground stations while SUHI is often observed using remote sensing methods. Recent advances in thermal imaging and remote sensing technology allowed the use of satellite and aircraft platforms (and recently drone platforms) (Dvorský, Snášel and Voženílek 2009). Nowadays, UHI studies can combine thermal remote sensing data with urban micrometeorology. This approach brings new opportunities but also new challenges. Voogt and Oke (2003) state that the emphasis on proper and precise definitions of various phenomena is crucial in advancements of this field.

Thermal remote sensing measures emitted radiation by the surface which incorporates effects of the surface such as surface moisture, thermal admittance, emissivity, sun and atmospheric irradiance and the effects of the near-surface atmosphere. We use the term directional

DOI: *https://doi.org/10.33542/GC2020-1-05*

brightness temperature to describe the temperature calculated using the inversion of Plank's law using a certain thermal sensor that operates at a certain wavelength. After the data are corrected for atmospheric effects and surface emissivity, we talk about directional radiometric temperatures.

Understanding the characteristics of surfaces is important for further work with local variability (Vozenilek et al. 2012). Spatial phenomena such as roof or vegetation geometry, building height and others affect remotely sensed data in a major way. According to Zemek (2014), thermal remote sensing measurements are affected by two main sources: the atmosphere and the measured surface. While atmospheric corrections are rather well established due to other remote sensing applications, we cannot say the same about the thermodynamic properties and geometry of the surface. Emissivity corrections can be applied easily when the surface material is known to the researcher. On the other hand, the geometry of the object and the effect of thermal anisotropy are not that easy to remove. Various models are trying to predict this phenomenon and improve thermal images.

Oke et al. (2017) described the correlation between surface temperature and air temperature at UCL as a possible result of micro-advection caused by increased surface temperature. For the night-time case of the UHI, surface – air temperature differences are expected to be minimised as winds increase, due to mixing and disruption of any surface-based inversion layer. Under calm winds and clear skies, when the UHI has its best expression, micro-scale processes dependent on surface thermal properties, sky view factor and microscale advection will be most apparent thereby increasing differences between the UHI and SUHI.

As the main disadvantage of using thermal remote sensing data in urban climate models is according to Voogt and Oke (2003) the difference between surface temperature and the aerodynamic temperature needed for the calculation of the surface sensible heat flux.

Urban heat island, a term used since 1940s (e.g. Balchin and Pye 1947), was researched in depth by Sundborg (1952), who articulated his theory about urban energy balance based on the incoming and outgoing energy flux balance. He further elaborated, that the energy absorbed by the urban surface system from solar radiation and generated by anthropogenic activity is physically balanced by warming the air above the surface, the evaporation of moisture, and storage of heat in surface materials.

Oke (2003) pointed out that UHI can be observed on two different levels. Urban Canopy Layer (UCL) describes the air mass between the surface and approximate mean building height, while Urban Boundary Level (UBL) lays above the canopy layer and is affected by the upward urban effect. For UCL measuring, regular measurement in meteorological height or vehicle-mounted sensors is sufficient to model this phenomenon. However, Chrysoulakis et al. (2016) suggest UBL specialised sensor platforms for proper measurements at UBL. A special case of UHI called Surface Urban Heat Island is observed by remote sensing platforms. However, analysis of this phenomenon must be carried out with caution because of the specific regime of various materials.

While anthropogenic heat flux along with anthropogenic materials contributes the most to the urban heat island effect, Gunawardena et al. (2017) suggest green-spaces and blue-spaces as the natural countermeasure. In their meta-analysis, they suggest careful urban planning heavily based on urban modelling to mitigate the UHI effect.

Leading applications in thermal infrared remote sensing

Thermal Infrared (TIR) remote sensing has numerous applications in different geographical topics. In physical geography, the examples are natural resources detection using thermal spectroscopy (Schlerf et al. 2012), arctic region monitoring (Soliman et al. 2012), soil property research using thermal and visible spectral region data fusion (Eisele et al. 2012) or research in water quality and fisheries management using stream temperature acquired by airborne

remote sensing (Torgersen et al. 2001). Due to recent droughts in Amazon forest, Jiménez-Muñoz et al. (2016) were investigating the possibilities of using MODIS and ERA-Interim products to understand forest response and potential impact on carbon absorption. Sepulcre-Cantó et al. (2006) suggest water stress detection in non-homogeneous crop canopies as another possible application.

TIR remote sensing is also extremely beneficial in urban studies, especially regarding (surface) urban heat island, urban modelling and heat comfort. TIR remote sensing is beneficial in urban heat budget studies (Parlow 2003) which then overlap with urban heat flux modelling. (Rigo and Parlow 2007). It can also help the property owners and communities regarding urban energy efficiency and insulation quality assessment (Hay et al. 2011) or help with spatial planning (Jovanović et al. 2015).

Most importantly, TIR remote sensing is used for detection, evaluation and monitoring of urban heat island (UHI) effect including assessment of surface urban heat island. (e.g., Weng 2009) Many studies utilize satellite imagery (Weng 2009, Majkowska, Kolendowicz and Pó 2017, Xiao et al. 2018), airborne imagery (Koc et al. 2018) and even temperature modelling (Feranec et al. 2016b).

The aim of this paper is to explore new possibilities of analysis for extreme resolution thermal imagery acquired from an aeroplane. For this purpose, the paper proposes four analyses including land cover class regime, verticality analysis, Local Climat Zones (LCZ) utilization and use of European open datasets.

Data

The main dataset used in this work consists of two raster datasets representing airborne campaigns over the city of Olomouc (Fig. 1) and surrounding area on 10th July 2016. The flight campaigns took place in the early morning and in the afternoon to maximise the lowest and highest temperatures during the day-night cycle.

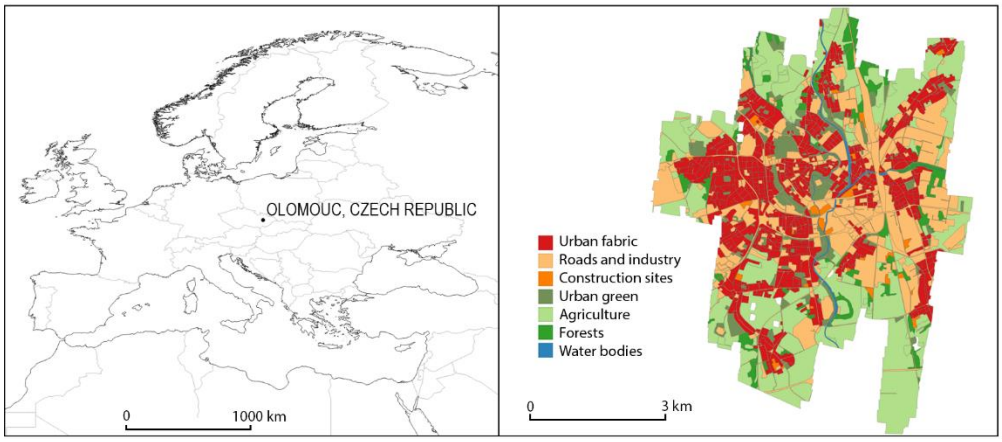

Fig. 1. *Location of the city of Olomouc in Europe (left). Urban Atlas classes of the area of interest (right)*

The carrier was Cessna 172 mounted with a photogrammetric sensor Phase One iXA-R 180 and thermal sensor Workswell Thermal Vision Pro based on FLIR Tau2 core. The average flight height was 769 m resulting in 90-100 cm pixel resolution. The area of interest was about 10 km × 8 km in size and was covered by 22 flight lines. Each flight took about 180 minutes and consisted of about 2100 images. The morning flight began at 0500 CEST and the afternoon flight at 1500 CEST (Fig. 2). The afternoon flight was scheduled at peak surface temperatures shortly after the meridian which for Olomouc is about 1300 CEST.

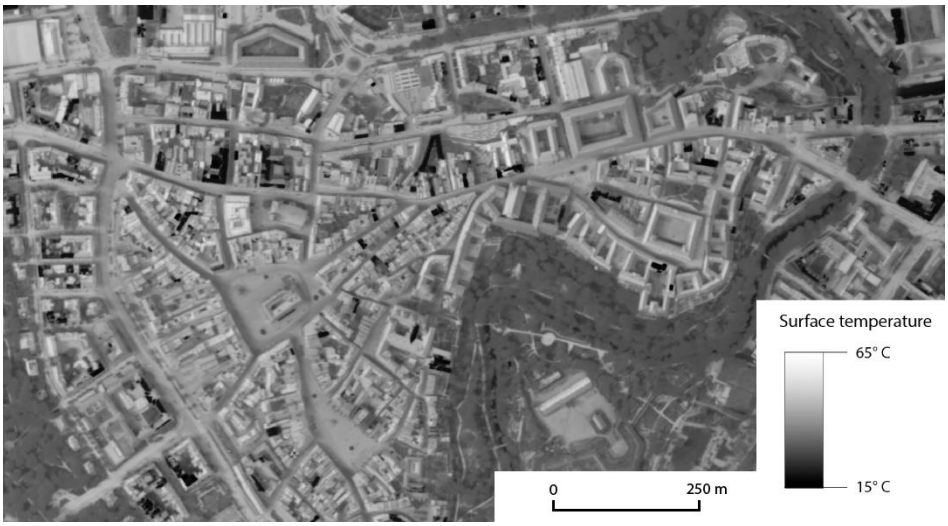

Fig. 2. *Visualisation of the afternoon thermal mosaic of Olomouc city centre*

The post-processing was consisting of vignetting removal, radiometric corrections, atmospheric corrections and emissivity corrections (Pour, Miřijovský and Purket 2019). In the final step, photogrammetric processing was applied to geo-reference the images and create a seamless thermal mosaic. The dataset consists of morning and afternoon mosaics, both in degrees Kelvin and Celsius. Along with the flight campaign, a ground truth measurement was performed using a FLIR E60 hand-held camera. The average error for various materials was under 1 °K; slightly larger for heterogeneous materials (asphalt) and objects with low accessibility (water).

Auxilliary datasets

The building dataset comes from the governmental Registry of Territorial Identification, Addresses and Real Estate (RÚIAN). The system was fully established on 1st July 2012 and is since then serviced by State Administration of Land Surveying and Cadastre (ČÚZK). It is a Czech national system collecting data originally stored in multiple systems. The initial data that filled the system came from Information System of the Cadastre of Real Estate (ISKN), Register of Census Districts and Buildings (RSO), Territorial Identification Registry of Addresses (UIR-ADR), Database of Deliver Sites of Czech Post (DDM) and Registry of Municipal Symbols (REKOS). The system is freely accessible through various means such as Public Remote Access (VDP), Information System of Territorial Identification (ISÚI) or service Atom operated by ČÚZK. In this thesis, data were downloaded using ArcGIS plugin named VFR Import. The plugin was created by company ARCDATA PRAHA, and its basic version is available free of charge. The RÚIAN dataset consists of many different layers in many vector types. For example, the layer of built-up objects used in this thesis is available as both point and multi-polygon layer.

The dataset was significantly enhanced by Tuháček (2017). The database was corrected for some errors and filled with missing features resulting in a total of 18 627 building objects. The height of the buildings was calculated based on the 5th Generation Digital Terrain Model of the Czech Republic (DMR 5G) and 1st Generation Digital Surface Model of the Czech Republic (DMP 1G). The difference of the models was added to the polygon layer attribute table.

Multiple errors forbid the immediate use of the data. These obstacles come from the specifics of the airborne campaign and the RÚIAN data. The data contain information only about the building footprint; therefore, in some cases, it does not precisely represent the rooftop

layer. Another problem was the quality of the mosaic. The spatial accuracy of the mosaicking process was very bad in certain parts of the image due to multiple issues within the processing chain. The errors caused significant spatial offset especially in the western part of the image.

Furthermore, the image suffers heavily from the skewing effect of tall buildings which creates offset increasing with building height. For these reasons, the dataset was manually edited, and the offset was adjusted to the afternoon thermal mosaic. Additionally, some buildings had to be manually added because they were either still missing from RÚIAN dataset due to outdated information or are not supposed to be part of it all.

Urban Atlas (UA, Urban Atlas 2019) is a tremendously unique dataset. It is a Europe-wide mapping service under European Space Agency Copernicus programme monitoring the land-use and land-cover changes over Large Urban Zones (LUZ). For the year 2006, there were 319 LUZs defined for the analysis, including cities with more than 100 000 inhabitants. In the year 2012, the number grew to 785 cities including EU28, EFTA and West Balkans countries and Turkey. The dataset is limited by minimal mapping unit (MMU). The MMU for 17 urban classes is 0.25 ha, while for ten rural classes the MMU is 1 ha. The methodology consists of Earth Observation (EO) data interpretation enhanced by topographic maps and auxiliary information including local expertise.

Moreover, the dataset also has auxiliary datasets; namely change detection between 2006 and 2012, Street Tree Layer (STL), building heights (2012 dataset only) and population estimates. However, these auxiliary data are provided only for some cities. All these datasets are accessible after free registration at Copernicus Land Monitoring Service webpage (land.copernicus.eu).

CORINE Land Cover (CLC, CORINE Land Cover 2019) is another great and ambitious source of data. The creation of this dataset was initiated in 1985 for the first reference year 1990. Since then, four more datasets (2000, 2006, 2012 and 2018) were created. CLC classification consists of 44 classes with minimal mapping unit of 25 ha for areal and 100 m minimal width for linear phenomena. The dataset is produced by most countries by visual interpretation of high-resolution satellite imagery. The production time of the dataset was reduced from 10 years (1990) to just about one year (2018). The number of countries was also increased from the original 26 to 39 in the latest dataset. CLC 2018 has the same overlay and access for download as Urban Atlas, requiring only free registration (Feranec et al. 2016a). It is available for the whole 39 countries as 100 m resolution GeoTiff (under 200 MB), SQLite Database (3.3 GB) or ESRI Geodatabase (1.7 GB). Along with the datasets from mentioned years, CLC also contains LULC change data labelled as "CHA" in the file structure. These change datasets are generated for every two following datasets, e.g. 2006-2012.

A dataset including a few vector layers was provided by Department of Urban Planning and Architecture of Olomouc city. Layers used in this research were road material type and lawn registry. The road material type layer is a vector layer distinguishing more than 20 road material types used within the city borders. These 20 classes were generalized into 5 classes – asphalt concrete, macadam, cobblestone, gravel and concrete. The lawn registry is a layer serving for the maintenance of public spaces and was used in the research to distinguish vegetation into "trees" and "grass" classes.

Methods and results

Thermal regime of land cover classes in an urban environment

The values of temperatures and their difference in between the times of the day were investigated. The sampling was based on auxiliary data from the city's municipality. The data contained information about specific road material type, so a more accurate typology and sampling could have been performed.

The road material class was further divided into the five most common material types. Road material classes are *asphalt concrete, macadam, cobblestone, gravel, and concrete*.

The asphalt concrete class is covering the majority of the roads in Olomouc and represents more than 90% of the area. Macadam is used mainly for parking lots, cobblestone in the historical centre of the city, gravel was found in the suburbs used for utility roads, and pure concrete was identified in several industrial areas.

The class containing natural objects was further divided into several subclasses. These are *grass, bare soil, tree crowns, agricultural crops*. The grass material was sampled based on another auxiliary dataset containing information for Technical Services of the city of Olomouc, helping them with effective watering. Tree crowns class was identified based on the optical imagery combined with the Digital Surface Model (DSM). Agricultural crops were differentiated from bare soil class based on the Normalized Difference Vegetation Index (NDVI).

Water bodies were distinguished on topographic maps of the area and in OpenStreetMap data. There are two small lakes close to the city, Hamrys and Morava's oxbow lake. Two main rivers, Morava and Bystřice, were identified, and more samples than in the preliminary study were gathered. The Trusovicky brook is a very small stream flowing into the Morava river before reaching the city. Morava arm is a part of the river that separates from the main river in northern part of the area and reconnects with the main stream within the city.

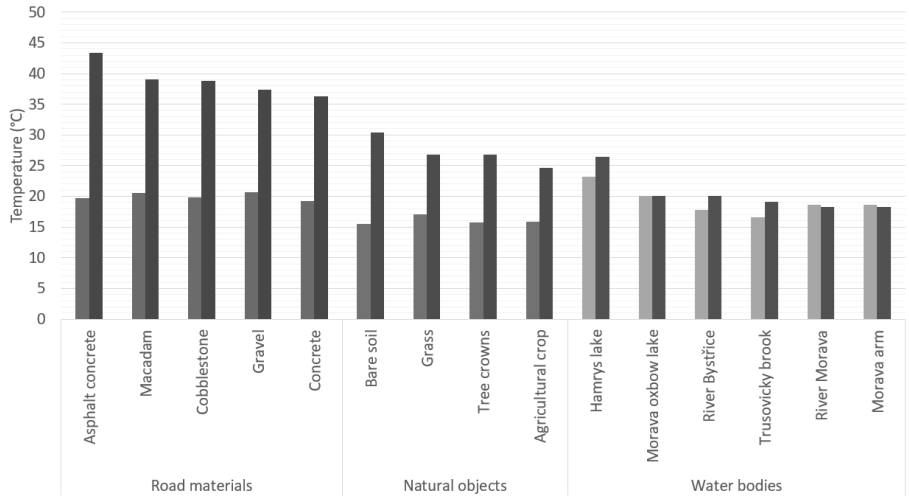

Fig. 3. *Thermal regime of various land cover classes in the city of Olomouc*

The results of the analysis are visualized in Figure 3. The subclasses within their respective groups are sorted descending based on their afternoon temperature for better orientation. The asphalt concrete material is easily recognized as the one with the largest afternoon temperature as well as the temperature difference between the morning and the afternoon. It heats about 10% more than the other road materials.

All the natural objects have very low morning temperature and tend not to heat up as much as the artificial ones. For example, in the afternoon, the grass material class is about 40% cooler than the asphalt concrete. Within the natural objects, the bare soil is approximately 5°C hotter than the other materials due to bare soil absorbing a large portion of the incoming EM radiation while plants use the energy for photosynthesis.

The water bodies group shows some very interesting information as well. The most significant is the Hamrys lake, which is a still water body prone to incoming EM radiation. The difference between the rivers Morava and Bystřice is the same as described in the preliminary results section. Morava's oxbow lake is a very interesting phenomenon as it does not change its temperature at all throughout the day. The Trusovicky brook is a very shallow and fast stream, and its thermal behaviour is similar to the Bystřice river.

Investigation of temperatures on different vertical levels

Verticality is a very important factor in urban climate research. One of the crucial paradigms regarding the quality of life within the city and the effect of long-wave irradiation on humans is that people live in the streets, not on the rooftops. Having a small to medium resolution thermal satellite images provides us with information about the temperature of the city surface. However, these data tell us only a little about the inner structure of the city. The denser the city is, the stronger the UHI effect might appear in comparison to a rural area. The effect is caused mainly by materials used for rooftops. Another example of factors contributing to the temperature difference between the rooftop and the ground level are shadows and vegetation. On the contrary, the rooftop level should not be affected by city canyons, upwelling radiation and should be ventilated much more effectively. In this chapter, GIS tools are used to investigate the various possible hypothesis.

Regarding the difference between ground and rooftop verticality levels, the results show a very significant difference (Fig. 4). In the morning, most of the materials share similar temperature around 17.5°C because of the night cooling effect. In the afternoon, however, the rooftop level shows a drastic increase of 18.44°C in comparison to ground level 12.62°C. To summarise, within the observed timeframe, rooftop materials heated up on average 46% more than ground level materials. These results prove the high importance of very high-resolution or down-scaled data providing context for city surface temperature.

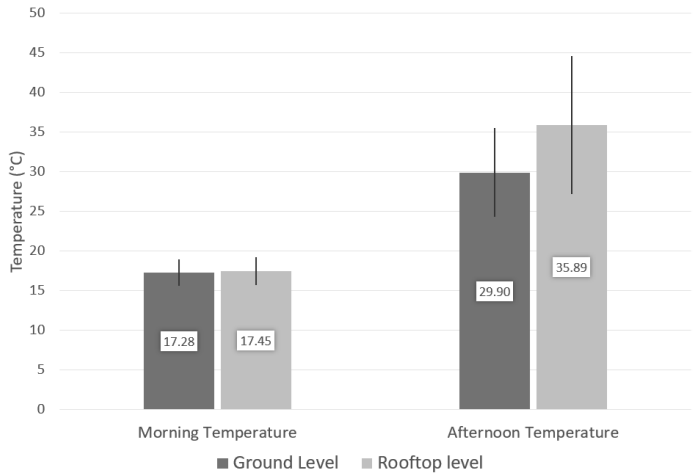

Fig. 4. *Comparison of temperature means on different vertical levels*

The second hypothesis regarded the connection between roof temperature and the building height. Multiple characteristics affect the air temperature in higher urban levels and the actual temperature of the material. In general, the temperature should be lower due to better ventilation and lower air temperature tied to a higher altitude. There are many other factors tied to the measured material. Besides the material type, the temperature is also affected by the age of the material, corrosion or kind of other damage, temporal cover such as moss or other vege-tation and so on. The question asked was whether the correlation between the material temperature and the height is significant. The original dataset of more than 15 000 building objects was filtered to be more easily visualised. The outliers were removed first, especially buildings errors such as with negative height. After that, the buildings that were missing either the temperature or the height parameter were filtered. In the last step, all buildings below 10 metres of height were removed. Most of these buildings were outdoor garages, various shacks, temporary buildings and others. The remaining approximately 5000 buildings were analysed and visualised (Fig. 5 and Fig. 6).

In both graphs, the values for tallest buildings are cut off for better visibility. However, those values were included in the calculation. In the afternoon dataset (Fig. 5), where there is a larger contrast between various materials, the Pearson's product moment correlation coefficient of 0.06 has been calculated. Moreover, linear regression shows no visible trend in the data.

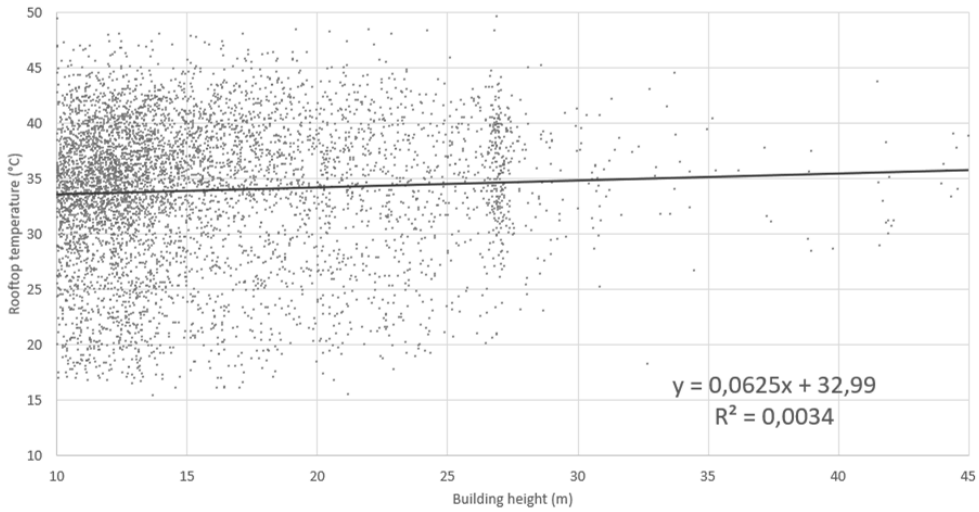

Fig. 5. *Afternoon rooftop surface temperature at different building height levels*

The morning dataset shows much bigger consistency (and less contrast) of temperatures due to night-time cooling effect, and thus it was less probable to find any clear trend in the dataset (Fig. 6). The Pearson's product moment correlation coefficient of the two variables equals -0.05. In combination with the linear regression, there is no clear connection between the building height and the rooftop temperature.

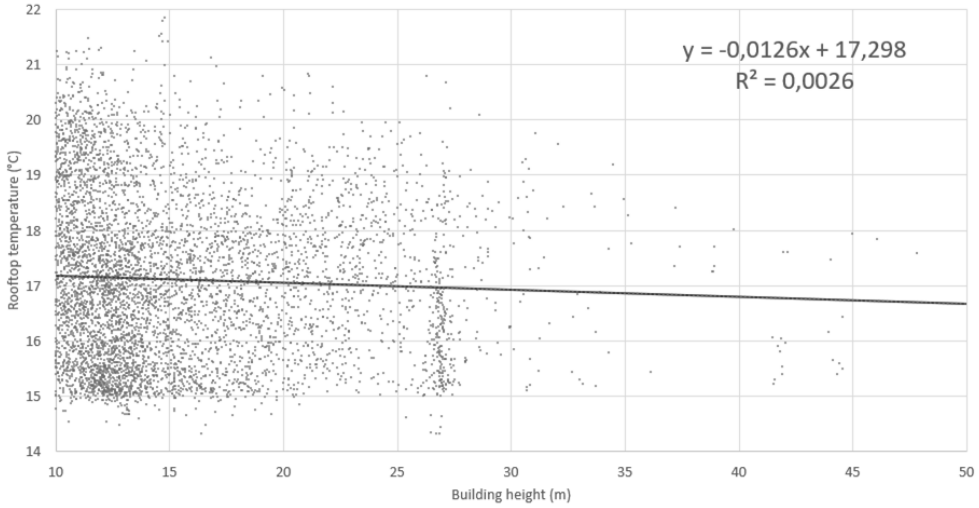

Fig. 6. *Morning rooftop surface temperature at different building height levels*

In conclusion, the height attribute does not have any clear impact on the rooftop material temperature. While there possibly is some impact, the other attributes affecting the temperature are probably much more significant for the measurement.

Temperature evaluation based on open data

UA 2012 dataset features 21 classes in the city of Olomouc, which are represented by a 5-digit code. Three of these classes contain 67% of the area. These are 21000 – Arable land (28%), 12100 – Industrial, commercial, public, military and private units (21%) and 11100 – Continuous urban fabric (18%). Nine of the classes are heavily under-represented, having less than 1% of the total area. These classes are summarized as other in Figure 7 and visualised as outlines in 7.11. Even though they have a small size, some of them are still notable in logical analysis. Especially 12400 – Airports and 12210 – Fast transit roads cannot be excluded from the overall picture.

The mean temperatures read from the afternoon and morning datasets are visualised in Figure 7. Morning average temperatures range approximately between 15 and 20°C while afternoon means range from 23 to 35°C. The Land-use/Land-cover (LULC) categories are sorted by the ID number and their respective super-categories. There is a total of seven classes that are under-represented in the image (under 0.5% of the total area; visualised in lower opacity). Water shows the typical behaviour of a material with high thermal inertia having the second highest morning temperature of 18.21°C while having significantly lowest afternoon temperature of only 23°C. There is a visible border between natural and artificial materials at 30°C. Classes 1.4, 2, 3, and five are having a mean afternoon temperature under 30°C while all artificial classes 1.1, 1.2, and 1.3 have mean over 30°C.

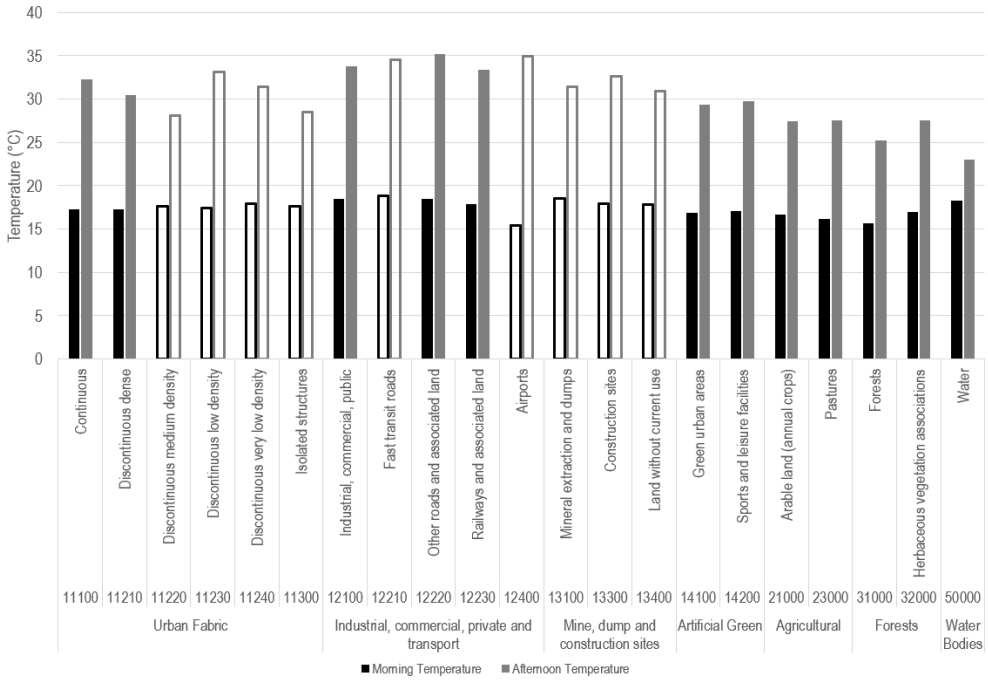

Fig. 7. *Morning and afternoon temperature of Urban Atlas 2012 classes in the city of Olomouc; Classes visualized as outlines are under-represented in the dataset, their area is lower than 1% of the total area*

The CLC 2018 dataset for the city of Olomouc consists of 14 classes. Three of the classes add up to 80% of the whole area. These are 112 – Discontinuous urban fabric (35%), 211 – Non-irrigated arable land (29%) and 121 – Industrial and commercial (16%).

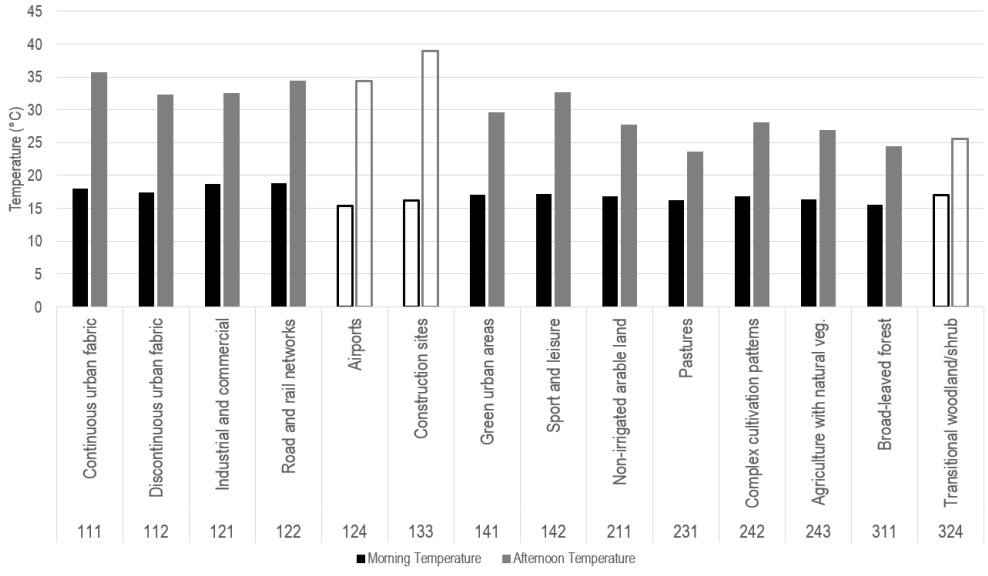

Fig. 8. *Morning and afternoon temperature of CORINE Land Cover 2018 classes in the city of Olomouc; Classes visualized as outlines are under-represented in the dataset, their area is lower than 1% of the total area*

Three of the classes were under-represented, specifically Airports (code 124), Construction sites (code 133) and Transitional woodland and shrub (code 324). These classes have under 1% of the total area, are summed up into the class other in and are visualised only as an outline in Figure 8.

The highest afternoon surface temperature was measured on construction sites (class 133) followed by airports (124), continuous urban fabric (111) and road and railway networks (122). An interesting fact is that airport class is among the hottest in the afternoon but has very good cooling capability during the night resulting in low morning temperature. This is most probably caused by the elevated position of the airport combined with its open space providing great ventilation.

Traditionally, natural surface classes account for the lowest afternoon temperature, broad-leaved forest (311) and pastures (231) heating up to less than 25°C. Surprisingly high are the green urban areas (141) having average afternoon surface temperature of almost 30°C. The reason here is probably coarse spatial resolution of the CLC dataset, so the green urban area class consists also of surrounding streets and buildings neighbouring the actual parks.

Local Climate Zones and the analysis of neighbourhoods

The principle of Local Climate Zones (LCZ) was firstly presented by Stewart and Oke (2012). LCZs are supposed to be the answer for urban statistical analysis as they set a basic unit of comparison. Authors have created a methodology based on built-up area, sky view factor, building height, vegetative fraction and other factors. From the point of climatology, LCZs are relatively homogeneous areas (neighbourhoods) of size in between $10^2 \times 10^2$ and $10^4 \times 10^4$ metres. The main strength of LCZs is the possibility of comparing similar data from different regions and creating metadata information for meteorological and climatological data.

Due to the absence of reliable Digital Surface Model (DSM) for Sky View Factor (SVF) and average building height calculations, we have decided to classify the classes manually based on satellite imagery and local knowledge of the city. The classification was based on the

written description of the classes in Stewart and Oke (2012). 47 LCZs were identified; eight were not classified as they had very specific land-use/land-cover mixture and could not be classified easily. One of the examples is the area around football stadium which contains an outdoor swimming pool, three football fields with tribunes, several tennis courts, some low-rise and mid-rise buildings as well as multiple high-rise hotels. Following the LCZ methodology, the climatic characteristic of this area is unclear.

We evaluated this process based on building and vegetation fractions that were calculated for these areas and are presented in Figure 9. LCZ2 (Compact midrise) is showing very large building fraction and only a little vegetation which is typical for continuous built-up area. On contrary, LCZA (Dense trees) contains almost no building fraction and consists of more than 60% of vegetation. LCZG (Water bodies) shows some vegetation fraction mainly because of the riverside areas. Industrial areas were classified as LCZ8 (Large lowrise) and show high fraction of buildings while having only small fraction of vegetation. Classes LCZ4, LCZ5 and LCZ6 are representing open areas of highrise, midrise and lowrise buildings respectively. It is worth noting that the LCZ6 has significantly higher vegetation fraction on average than the other classes even though the building fraction remains roughly the same.

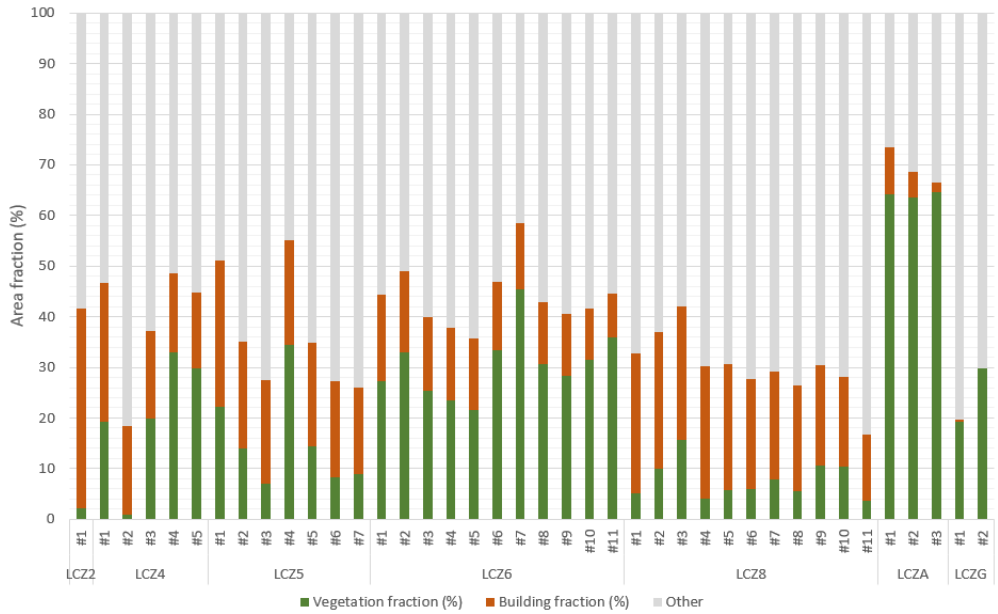

Fig. 9. *LCZs characteristics based on the vegetation and building fractions complemented to 100% by the class 'other'*

While the building and vegetation fraction analysis showed some interesting facts about residential and industrial areas in Olomouc, the most important part of this analysis was its relation to the surface temperature. In Figure 10, the temperature of different LCZs is visualised. For easier interpretation, vertical lines visualising temperature change between the morning and the afternoon temperatures are used. Moreover, horizontal dashed lines are representing the mean morning (lighter line in the bottom) and afternoon (darker line on top) temperature within certain LCZ type for easier visual comparison of the LCZ types as they have large variability. Open low-rise (LCZ6) seems to be the best area in terms of temperature regime among residential areas which corresponds with high vegetation fraction discussed previously. It is important to emphasise that the average afternoon surface temperature of the other residential zones (LCZ2, LCZ4, and LCZ5) is the same or higher than the temperature of industrial areas (LCZ8).

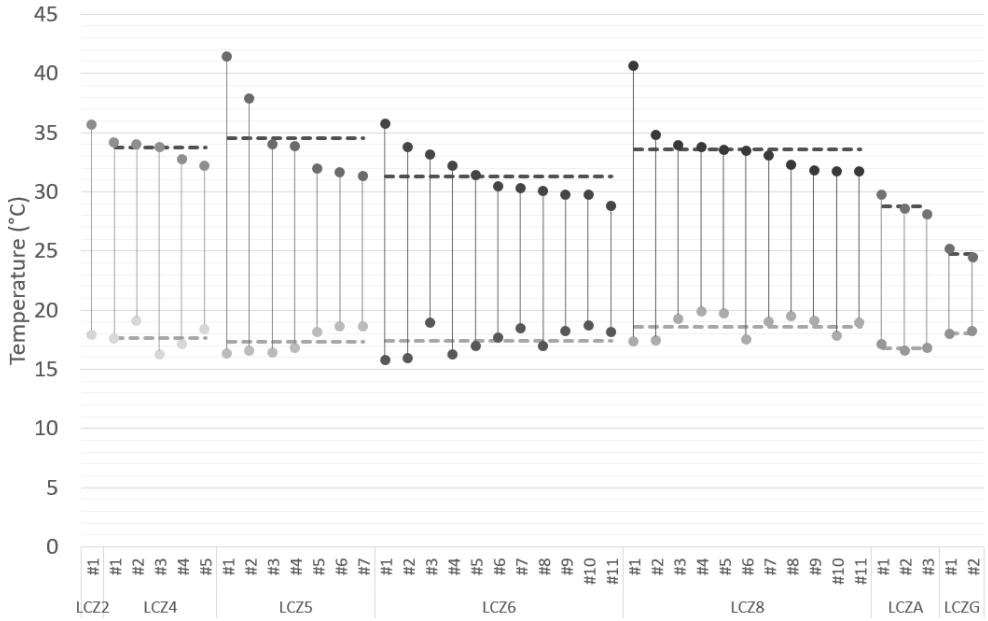

Fig. 10. *Mean temperature of LCZs in the city of Olomouc*

Discussion

The results of the LCZ analysis can be compared with the results of Koc et al. (2018). The LCZ8 class was among the warmest in both studies during the day. In Olomouc, the coldest surface throughout the day was water while in their data from Sydney it was LCZA, dense forrest. Very different results appear during the night when in Olomouc, the water cools relatively well and the industrial zones fail to cool down. Koc et al. (2018) reports that water remains the warmest surface and the industrial zones are among the coldest. It would be very interesting to research the connection in thermal behaviour of LCZs in various regions more in depth, especially on cases such as Sydney and Olomouc.

Probably the closest research to our open data analysis was done by Xiao et al. (2018). They were acquiring surface temperature from Landsat 8 OLI over the cities of Vienna, Austria and Madrid, Spain in similar time of the year in 2013. Their time window was slightly different as the time of acquisition for Vienna was 1105 CEST and 1245 CEST for Madrid. Their estimation of surface temperature of almost 36°C corresponds to our measurement in the same class of 32.5°C. Water temperature is also very similar having 27°C in Vienna and 23°C on our measurement. From the presented results is clear that the thermal regime of Vienna is very similar to our results from Olomouc while Madrid results differ in many aspects, especially the temperature of vegetation and the fact that with decreasing building density the average temperature of the class remains similar.

Conclusions

The article aimed to present original types of analysis of extreme resolution thermal data. Overall four types of analyses were proposed. Analysis considering vertical parameter using RÚIAN data provided an interesting insight into the difference between ground level and rooftop level; rooftop material is heating up on average 46% more than the ground level materials. Moreover, there was no relation proved between the exact height of a building and the temperature of the roof. The dataset was further compared to Europe-wide open datasets Urban

Atlas 2012 and CORINE Land Cover 2018. In these datasets, artificial classes showed much higher afternoon temperature, on average above 30°C; while natural land use classes were significantly cooler. The additional analysis focused on manually collected samples of various materials. Its results show the largest heat up the effect of socialist-era apartment buildings despite the high-quality ventilation and relatively lower air temperature. The temperature regime difference between slow-paced deep river Morava and fast-paced shallow stream Bystřice was observed. River Morava showed much higher thermal inertia resulting in lower afternoon temperature and lower night-time cooling effect resulting in higher morning temperature. In the last analysis, LCZs as the source of reference units was investigated. Multiple LCZs were manually classified and investigated. The results showed variety not only in between the classes but also within the LCZ types around the city.

The article shows multiple possibilities of data fusion to analyse urban landscape from the perspective of thermal dynamics. Verticality is an important factor that needs to be taken into account when considering the quality of life and heat within the city. Open data in the form of CORINE Land Cover and Urban Atlas are a very useful basis for inter-city comparison of the results. Local Climate Zones further increase the possibility of both inter-city and intra-city comparison of thermal behaviour of urban surfaces.

To conclude, extreme resolution thermal images open up many possibilities of analysis suitable especially for monitoring over long periods or over multiple cities at the same time.

References

BALCHIN, W. G. V., PYE, N. 1947: A micro-climatological investigation of bath and the surrounding district. *Quarterly Journal of the Royal Meteorological Society*, 73(317-318), 297-323. DOI: https://doi.org/10.1002/qj.49707331706.

CHRYSOULAKIS, N. et al. 2016: A novel approach for anthropogenic heat flux estimation from space. 2016 IEEE International Geoscience and Remote Sensing Symposium, pp. 6774-6777. DOI: https://doi.org/10.1109/IGARSS.2016.7730768.

CORINE LAND COVER 2019: *Copernicus Land Monitoring Service*. [cit. 2019-05-28]. Retrieved from: https://land.copernicus.eu/pan-european/corine-land-cover.

DVORSKÝ, J., SNÁŠEL, V., VOŽENÍLEK, V. 2009: Map similarity testing using matrix decomposition. In Badr, Y., Caballé, S., Xhafa, F. et al. eds. *International Conference on Intelligent Networking and Collaborative Systems, INCoS 2009*. Barcelona (IEEE Computer Society), pp. 290-294, DOI: https://doi.org/10.1109/INCOS.2009.74.

EISELE, A. et al. 2012: Applicability of the thermal infrared spectral region for the prediction of soil properties across semi-arid agricultural landscapes. *Remote Sensing*, 4(11), 3265-3286. DOI: https://doi.org/10.3390/rs4113265.

FERANEC, J. et al. 2016a: *European Landscape Dynamics: CORINE Land Cover Data*. Boca Raton (CRC Press). DOI: https://doi.org/10.1201/9781315372860.

FERANEC, J. et al. 2016b: Influence of land cover / land use changes on urban heat island: Case study of Bratislava. *IGU-LUCC Research Reports*, 13, 29-42.

GUNAWARDENA, K. R., WELLS, M. J., KERSHAW, T. 2017: Utilising green and bluespace to mitigate urban heat island intensity. *Science of the Total Environmen*t, 584-585, 1040-1055. DOI: https://doi.org/10.1016/j.scitotenv.2017.01.158.

HAY, G. J. et al. 2011: Geospatial technologies to improve urban energy efficiency. *Remote Sensing*, 3(7), 1380-1405. DOI: https://doi.org/10.3390/rs3071380.

JIMÉNEZ-MUÑOZ, J. C. et al. 2016: Digital thermal monitoring of the Amazon forest: an intercomparison of satellite and reanalysis products. *International Journal of Digital Earth*, 9(5), 477-498. DOI: https://doi.org/10.1080/17538947.2015.1056559.

JOVANOVIĆ, D. et al. 2015: Spatial analysis of high-resolution urban thermal patterns in Vojvodina, Serbia. *Geocarto International*, 30(5), 483-505. DOI: https://doi.org/10.1080/10106049.2014.985747.

KOC, C. B. et al. 2018: Understanding Land Surface Temperature Differences of Local Climate Zones Based on Airborne Remote Sensing Data. *IEEE Journal of Selected Topics in Applied Earth Observations and Remote Sensing*, 11(8), 2724-2730. DOI: https://doi.org/10.1109/JSTARS.2018.2815004.

MAJKOWSKA, A., KOLENDOWICZ, L. AND PÓ, M. 2017: The urban heat island in the city of Poznań as derived from Landsat 5 TM. *Theoretical and Applied Climatology*, 128, 769-783. DOI: https://doi.org/10.1007/s00704-016-1737-6.

OKE, T. R. et al. 2017: *Urban Climates*. Cambridge (Cambridge University Press). DOI: https://doi.org/10.1017/9781139016476.

PARLOW, E. 2003: The urban heat budget derived from satellite data. *Geographica Helvetica*, 58(2), 99-111.

POUR, T., MIŘIJOVSKÝ, J. AND PURKET, T. 2019: Airborne thermal remote sensing: the case of the city of Olomouc, Czech Republic. *European Journal of Remote Sensing*, 52, 209-218. DOI: https://doi.org/10.1080/22797254.2018.1564888.

RIGO, G. AND PARLOW, E. 2007: Modelling the ground heat flux of an urban area using remote sensing data. *Theoretical and Applied Climatology*, 90, 185-199. DOI: https://doi.org/10.1007/s00704-006-0279-8.

SCHLERF, M. et al. 2012: A hyperspectral thermal infrared imaging instrument for natural resources applications. *Remote Sensing*, 4(12), 3995-4009. DOI: https://doi.org/10.3390/rs4123995.

SEPULCRE-CANTÓ, G. et al. 2006: Detection of water stress in an olive orchard with thermal remote sensing imagery. *Agricultural and Forest Meteorology*, 136(1-2), 31-44. DOI: https://doi.org/10.1016/j.agrformet.2006.01.008.

SOLIMAN, A. et al. 2012: Pan-arctic land surface temperature from MODIS and AATSR: Product development and intercomparison. *Remote Sensing*, 4(12), 3833-3856. DOI: https://doi.org/10.3390/rs4123833.

STEWART, I. D. AND OKE, T. R. 2012: Local climate zones for urban temperature studies. *Bulletin of the American Meteorological Society*, 93(12), 1879-1900. DOI: https://doi.org/10.1175/BAMS-D-11-00019.1.

SUNDBORG, A. 1952: *Geographica No. 22: Climatological studies in Uppsala with special regard to the temperature conditions in the urban area*. Uppsala (Uppsala Uniersitet), 111 p.

TORGERSEN, C. E. et al. 2001: Airborne thermal remote sensing for water temperature assessment in rivers and streams. *Remote Sensing of Environment*, 76(3), 386-398. DOI: https://doi.org/10.1016/S0034-4257(01)00186-9.

TUHÁČEK, T. 2017: *Floor area ratio of buildings in Olomouc – bachelor thesis*. Olomouc (Palacky University Olomouc).

URBAN ATLAS 2012: Copernicus Land Monitoring Service. [cit. 2019-05-28]. Retrieved from: https://land.copernicus.eu/local/urban-atlas/urban-atlas-2012.

URBAN ATLAS 2019*: Copernicus Land Monitoring Service*. [cit. 2019-05-28]. Retrieved from: https://land.copernicus.eu/local/urban-atlas.

VOOGT, J. A. AND OKE, T. R. 2003: Thermal remote sensing of urban climates. *Remote Sensing of Environment*, 86(3), 370-384. DOI: https://doi.org/10.1016/S0034-4257(03)00079-8.

VOZENILEK, V. et al. 2012: Orthophoto feature extraction and clustering. *Neural Network World*, 22(2), 103-121. DOI: https://doi.org/10.14311/NNW.2012.22.007.

WENG, Q. 2009: Thermal infrared remote sensing for urban climate and environmental studies: Methods, applications, and trends. *ISPRS Journal of Photogrammetry and Remote Sensing*, 64(4), 335-344. DOI: https://doi.org/10.1016/j.isprsjprs.2009.03.007.

XIAO, H. et al. 2018: Responses of Urban Land Surface Temperature on Land Cover: A Comparative Study of Vienna and Madrid. *Sustainability*, 10(2), 260. DOI: https://doi.org/10.3390/su10020260.

ZEMEK, F. 2014: *Airborne remote sensing: theory and practice in assessment of terrestrial ecosystems*. Brno (Global Change Research Centre AS CR).

Acknowledgement: This paper was created within the project "Innovation and application of geoinformatic methods for solving spatial challenges in the real world." (IGA PrF 2019 014) with the support of Internal Grant Agency of Palacky University Olomouc.

Authors' affiliations

Mgr. Tomáš Pour
Department of Geoinformatics
Faculty of Science, Palacký University in Olomouc
17. listopadu 50, 771 46 Olomouc
Czech Republic
pour.tomas@gmail.com

prof. RNDr. Vít Voženílek, CSc.
Department of Geoinformatics
Faculty of Science, Palacký University in Olomouc
17. listopadu 50, 771 46 Olomouc
Czech Republic
vit.vozenilek@upol.cz